University of Baghdad
College of Engineering
JOURNAL OF ENGINEERING

Journal of Engineering
journal homepage: www.joe.uobaghdad.edu.iq
Number 2 Volume 26 February 2020

Civil and Architectural Engineering

Flexural Behavior of Fiber Reinforced Self-Compacting Rubberized Concrete Beams

Dr. Ahmed S. Ali
Assist. Professor
College of Engineering-Nahrain University
E-mail: ahmed_sltn2007@yahoo.com

Tamara M. Hasan
M.Sc. Student
College of Engineering-Nahrain University
E-mail: eng.tamara1993@gmail.com

ABSTRACT

The massive growth of the automotive industry and the development of vehicles use lead to produce a huge amount of waste tire rubber. Rubber tires are non-biodegradable, resulting in environmental problems such as fire risks. In this search, the flexural behavior of steel fiber reinforced self-compacting concrete (SFRSCC) beams containing different percentages and sizes of waste tire rubbers were studied and compared them with the flexural behavior of SCC and SFRSCC. Micro steel fiber (straight type) with aspect ratio 65 was used in mixes. The replacement of coarse and fine aggregate was 20% and 10% with chip and crumb rubber. Also, the replacement of limestone dust and silica fume was 50%, 25%, and 12% with ground rubber and very fine rubber, respectively. Twelve beams with small-scale (L=1100mm, h = 150mm, b =100mm) were tested under two points loading (monotonic loading). Fresh properties, hardened properties, load-deflection relation, first crack load, ultimate load, and crack width were investigated. Two tested reinforced concrete beams from experimental work were selected as a case study to compare with the results from ABAQUS program (monotonic loading). These two reinforced concrete beams were simulated as a parametric study under repeated loading using this finite element program. The results showed that the flexural behavior of SFRSCC beams containing rubber was acceptable when compared with flexural behavior of SCC and SFRSCC beams (depended on load carrying capacity). Cracks width was decreased with the addition of steel fibers and waste tires rubber. An acceptable agreement can be shown between the results of numerical analysis and the results obtained from experimental test (monotonic loading). Insignificant ultimate load differences between the results of monotonic loading and repeated loading

Keywords: waste tire rubbers, micro steel fiber, rubberized concrete, ABAQUS program.

سلوك الانثناء للعتبات الخرسانية الذاتية الرص الممطة والمعززة بالألياف

أ.م.د احمد سلطان علي
قسم الهندسة المدنية - كلية الهندسة - جامعة النهرين

تماره ميثم حسن
قسم الهندسة المدنية - كلية الهندسة - جامعة النهرين

الخلاصة

يؤدي النمو الهائل في صناعة السيارات وتطويرها الي انتاج كميات هائلة من مطاط الاطارات. الاطارات المطاطية غير قابلة للتحلل في الطبيعة، مما ينتج عن ذلك مشاكل بيئية مثل مخاطر الحرق. في هذا البحث، تم دراسة سلوك الانثناء للعتبات الخرسانيه

*Corresponding author
Peer review under the responsibility of University of Baghdad.
https://doi.org/10.31026/j.eng.2020.02.09

Article received: 2/6/2019
Article accepted: 10/7/2019
Article published: 1/2/2020

الذاتية الرص المعززة بألياف الحديد والمحتوية على نسب وقياسات مختلفة من مخلفات اطارات السيارات و مقارنتها بسلوك الانثناء للعتبات الخرسانية الذاتية الرص والعتبات الخرسانية الذاتية الرص المعززة بألياف الحديد. تم استخدام الالياف الفولاذية الدقيقة (النوع المستقيم) مع نسبة الطول الى العرض 65 في الخلطات. تم استبدال جزء من الركام الخشن والركام الناعم برقائق المطاط والمطاط المفتت بنسب 20% و 10%، كما تم استبدال الغبار الجيري والسيليكا بالمطاط المطحون والمطاط الناعم جدا بنسب 50% و25% و12%. تم اختبار اثنتا عشره عتبه ذات مقياس مصغر(الطول 1100ملم، الارتفاع 150 ملم، العرض 100 ملم) تحت تحميل نقطتين مركزتين(حمل رتيب). تم التحري عن علاقة الحمل بالتشوه وحمل الشق الاول والحمل النهائي وعرض الشق. تم اختيار اثنتين من العتبات التي تم فحصها بالمختبر للمقارنة مع برنامج ABAQUS. تم محاكاة هاتين العتبتين تحت التحميل المتكرر بأستخدام هذا البرنامج. اظهرت النتائج ان سلوك الانثناء للعتبات الخرسانية الذاتية الرص الممططة والمعززة بألياف الحديد كان مقبولا عن مقارنته بسلوك الانثناء للعتبات الخرسانية الذاتية الرص والعتبات الخرسانيه الذاتية الرص المعززه بألياف الحديد. قل عرض الشقوق بأضافه الياف الحديد ومخلفات اطارات السيارات. اظهرت النتائج توافق جيد بين نتائج التحليل العددي والنتائج التي تم الحصول عليها من العمل المختبري. فروق طفيفة للحمل النهائي بين نتائج التحميل الرتيب والتحميل المتكرر.

الكلمات الرئيسية: مخلفات اطارات السيارات، مايكرو ستيل فايبر، الخرسانة المطاطية، برنامج الاباكوس

1. INTRODUCTION

The overstocked of waste materials is an unavoidable stage of all industrial and human activities. These wastes create significant environmental and economic problems around the world. Many advantages can be accomplished through waste recycling in other processes, like reduce energy consuming, solve problems of disposal, minimize the use of natural resources (fine and coarse aggregate) also, decrease the health hazards on human and other vital components, **(De Brito and Saikia, 2012**). The use of alternative materials in concrete opens a whole new range of possibilities in the construction industry. The behavior of self-consolidating rubberized concrete (SCRC) beam-column joints under monotonic loading containing steel fibers and replacing fine aggregate with shredded rubber were investigated by **(Ganesan, et al., 2013)**, the percentage of rubber was15% by volume of fine aggregate. The results showed that the addition of shredded rubber improves the behavior of beam-column joint, such as energy absorption ability and ductility. The results also showed the presence of steel fibers and rubber particles improves resistance of crack and load-carrying capacity. The behavior of eight beams with intermediate scale (1700mm × 200mm × 100mm) containing waste tire rubbers by using four types of concrete, normal concrete, rubberized concrete (RC), self-compacting concrete (SCC), and self-compacting rubberized concrete (SCRC) was presented by **(Najim and Hall, 2014)**, the replacement of fine aggregate was 14% for RC and 18% for SCRC with crumb rubber. They observed that using crumb rubber decreased the flexural capacity and flexural stiffness.

On the other hand, the deformability and absorption of energy increased with the crumb rubber increased. The flexural behavior of SCRC (self-compacting rubberized concrete) beams with full-scale (2440mm×250mm×250mm) was studied by **(Ismail and Hassan, 2015)**, the percentage of crumb rubber ranging from 5% to 15% by volume of sand (fine aggregate). The behavior of the specimens was evaluated by using load-deflection relation. The tests of beams showed that increasing the rubber content decreased the first crack load, stiffness, and density, but the percentage of crumb rubber up to 10% improved deformability, ductility, and toughness of tested beams with slightly reducing in the flexural capacity. Many researchers studied fresh and hardened properties of SCC containing waste tire rubbers. Fine aggregate was replaced with crumb rubber (5, 10, and 15% by weight of fine aggregate). Fresh tests (slump flow, V-shape, L-shape, U-shape, and J-ring) and hardened tests (compressive strength, splitting tensile strength, and flexural strength) were carried out at 7, 28 and 90 days of curing by **(Padhi and Panda, 2016)**. The results showed that the incrementation in the proportion of rubber decreases the workability of SCRC. The results also showed that the replacement of fine aggregate by rubber particles decreases the hardened properties such as compressive strength. The flexural strength increased when the

percentage of crumb rubber was 5%. **(Matar and Assaad, 2019)**, investigated the workability and strength of self-compacting concrete containing recycled aggregates and polypropylene fibers. Different SCC mixes containing 25% to 100% recycled aggregate (RCA) and 0.25% to 1.75% polypropylene fiber (PPF) were prepared. The results showed that the fresh properties decreased with RCA, and PPF content increased. The compressive strength increased slightly when PPF increased. The reduction in splitting tensile strength due to RCA can be overcome by using PPF.
The use of finite element analysis (FEA) has increased because of the progressing knowledge and capability of computer package and hardware. ABAQUS has two approaches for modeling concrete response; smeared cracking and damaged plasticity. A concrete damaged plasticity model is suitable for various loading conditions such as monotonic loading, cyclic loading, and dynamic loading. This approach takes into account the degradation of the elastic stiffness resulting from plastic straining both in compression and tension. From the reason mentioned above, the damage plasticity model has been used for analysis the steel fiber reinforced self-compacting rubberized concrete beams **(Chaudhari and Chakrabarti, 2012)**.
The main aim of the present study is to produce successful mixes of steel fiber reinforced self-compacting rubberized concrete (SFRSCRC) in fresh and hardened properties (using waste tires rubber). Also investigate the effect of using different percentages of waste tire rubber (20% and 10% by weight of aggregates, 50%, 25%, and 12% by weight of limestone dust and silica fume) on behavior of simply supported beams under monotonic loading with the consideration of the following: 1) Load and deflection at first crack 2) Load and deflection at failure 3) Ductility, flexural stiffness, and residual strength factor. The behavior of simply supported beams under repeated loading by using the finite element program (ABAQUS) is also investigated.

2. EXPERIMENTAL STUDY

2.1 Materials Properties

Ordinary Portland cement (type I) was utilized for all the mixes. Fine aggregate (zone 2) and coarse aggregate (maximum size10 mm) were used according to **(IQS. No. 45/1984)**. The fine and coarse aggregate has specific gravity 2.65 and 2.6, respectively. Grey powder (silica fume) and white fine material (limestone dust) were used as pozzolanic and filler materials. The results of chemical and physical tests of silica fume satisfied with the **(ASTM C1240-15)** requirements. Viscosity modifying admixture (VMA) with specific gravity 1:1 and PH value 6.5 was used to obtain water reduction, workability, and viscosity. Micro steel fiber with length of 13 mm, aspect ratio 65, volume fraction (Vf = 1.5%), and tensile strength 2600 MPa as shown in **Fig. 1**. Waste tire rubber was prepared with different sizes, (1.18-9.5) mm was used instead of coarse aggregate (chip rubber), (0.15-4.75) mm was used instead of fine aggregate (crumb rubber), 125 and 2.5 microns were used instead of limestone dust and silica fume (ground rubber and very fine rubber). The different sizes of rubber with specific gravity 1.78 and water absorption 2% were obtained from General Company for Rubber Industries and Tires/ Iraq **(Fig. 2)**. Two sizes of steel reinforcement (Ø6mm and Ø4mm) were used to reinforce the beams with yield tensile stress 520 and 565 MPa, respectively (According to the **(ASTM A496-02)**).

Figure 1. Micro steel fiber.

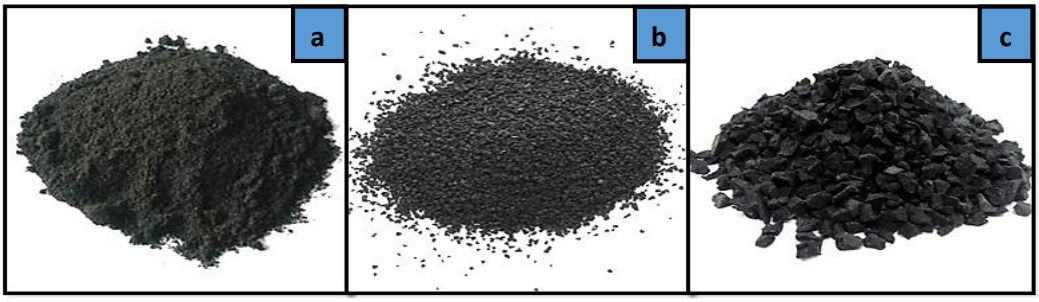

Figure 2. Types of tire rubber: (a) ground rubber, (b) crumb rubber, (c) chip rubber.

2.2 Concrete Mixes

It is very difficult to obtain successful mixes in fresh and hardened properties for SFRSCRC (steel fiber reinforced self-consolidating rubberized concrete); therefore, many trail mixes were conducted to obtain successful mixes in fresh characteristics for SFRSCRC (flowability and ability of passing) and the mixes were designed for structural concrete. The laboratory program includes the design of twelve types of mixes; (SCC, SFRSCC, SFRSCC with 20% and 10% of coarse aggregate was replaced by chip rubber, SFRSCC with 20% and 10% of fine aggregate was replaced by crumb rubber, SFRSCC with 50%, 25%, and 12% of limestone dust was replaced by ground rubber, and SFRSCC with 50%, 25%, and 12% of silica fume was replaced by very fine rubber. The details of the mixes used are listed in **Table 1**.

Table 1. Details of mixes.

Beam no.	Mixture	Cement	Natural aggregate		Rubber aggregate		Mineral admixture		Rubber		Steel fiber	VMA	Water
			Coarse aggregate	Fine aggregate	Chip rubber	Crumb rubber	Limestone dust	Silica fume	Ground rubber	Very fine rubber			
B1	SCC	400	810	890	-	-	60	80	-	-	-	14	153
B2	RSCC	400	810	890	-	-	60	80	-	-	117	16	186
B3	CA20	400	648	890	162	-	60	80	-	-	117	18	203
B4	CA10	400	729	890	81	-	60	80	-	-	117	17	195
B5	FA20	400	810	712	-	178	60	80	-	-	117	16	203
B6	FA10	400	810	801	-	89	60	80	-	-	117	15	200
B7	LS50	400	810	890	-	-	30	80	30	-	117	18	200
B8	LS25	400	810	890	-	-	45	80	15	-	117	17	190
B9	LS12	400	810	890	-	-	52	80	8	-	117	16	185

B10	SF50	400	810	890	-	-	60	40	-	40	117	16	186
B11	SF25	400	810	890	-	-	60	60	-	20	117	15	180
B12	SF12	400	810	890	-	-	60	70	-	10	117	14	169

*All quantities are in kg/m^3

Tests of Fresh Concrete

The tests of slump flow, V-funnel, and L-box were carried out to obtain successful mixes in fresh properties of SCC (flowability and ability of passing). The tests were carried out according to the European guideline for SCC **(EFNARC 2005)**. **Fig. 3** shows the tests of fresh concrete.

Figure 3. Fresh properties tests: (a) slump flow, (b) L-box, (c) V-funnel.

2.3 Tests of Hardened Concrete

At 28 days, the tests of compressive strength and splitting tensile strength were carried out by using (100×100×100) mm cube and (100×200) mm cylinder, according to **(BS 1881: part 116: 1997)** and **(ASTM C496-11)**, respectively. The modulus of the rupture test was also conducted by using (100×100×400) mm prism, according to **(ASTM C78-02)**.

2.4 Flexural Test Setup and Instrumentation

Twelve beams was reinforced with deformed bars, two (Ø6mm) for main reinforcement, and two (Ø4mm) for compression reinforcement. To prevent shear failure, (Ø4 @ 56mm c/c) was used. The dimensions of each beam were (L=1100mm, h=150mm, b=100mm). All beams were designed to fail in flexural according to **(ACI 318M-14)**. The beams were tested under two concentrated loads (monotonic load). The beam's designation and description are illustrated in **Table 2**. The dimensions of beam and details of reinforcement are shown in **Fig. 4**.

Table 2. Beams designation and description.

Beam no.	Beam designation	Description
B1	SCC	Self-compacting concrete
B2	RSCC	Steel fiber reinforced self-compacting concrete (SFRSCC) + (Vf =1.5%)
B3	CA20	SFRSCC + 20% of coarse aggregate replace by chip rubber
B4	CA10	SFRSCC + 10% of coarse aggregate replace by chip rubber

B5	FA20	SFRSCC + 20% of fine aggregate replace by crumb rubber
B6	FA10	SFRSCC + 10% of fine aggregate replace by crumb rubber
B7	LS50	SFRSCC + 50% of lime stone dust replace by ground rubber
B8	LS25	SFRSCC + 25% of lime stone dust replace by ground rubber
B9	LS12	SFRSCC + 12% of lime stone dust replace by ground rubber
B10	SF50	SFRSCC + 50% of silica fume replace by very fine rubber
B11	SF25	SFRSCC + 25% of silica fume replace by very fine rubber
B12	SF12	SFRSCC + 12% of silica fume replace by very fine rubber

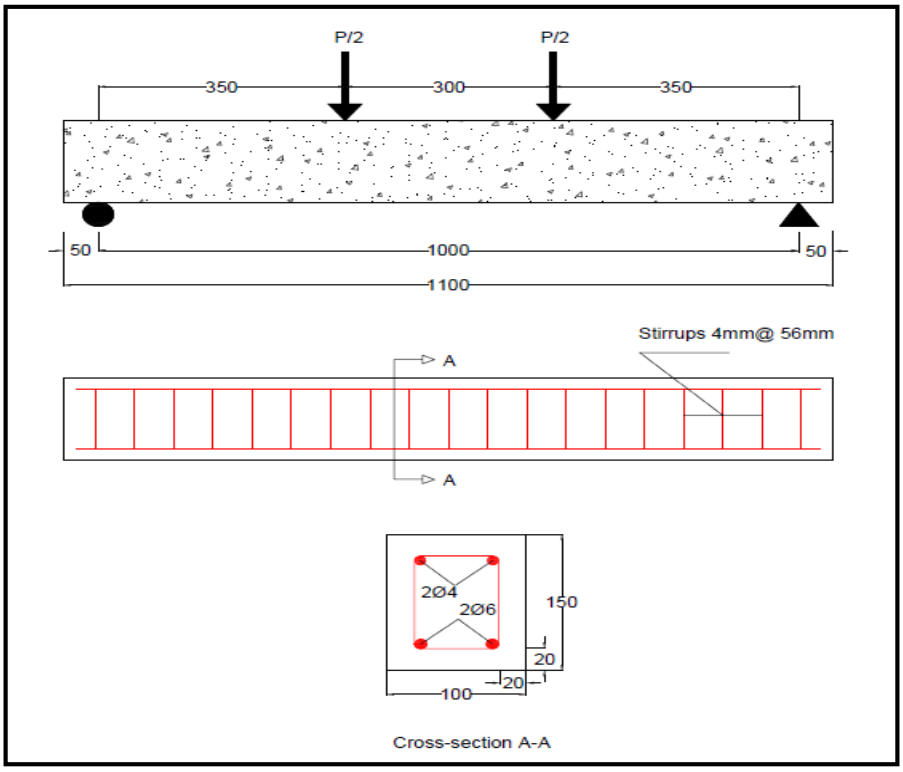

Figure 4. Beam dimensions and reinforcement details.

3. FINITE ELEMENT ANALYSIS

3.1 Element Type

The element types used for modeling the simply supported beams using ABAQUS software are summarized in the following sections:

3.1.1 Modeling of concrete

Beams are modeled using three-dimensional finite elements. Standard 3D stress elements in ABAQUS can be utilized for modeling of concrete**.** An 8-node linear brick (C3D8R element) is used to model concrete beams. The integration point of the C3D8R element is located in the middle of the element. **Fig. 5** shows the 8-node brick element with the integration point.

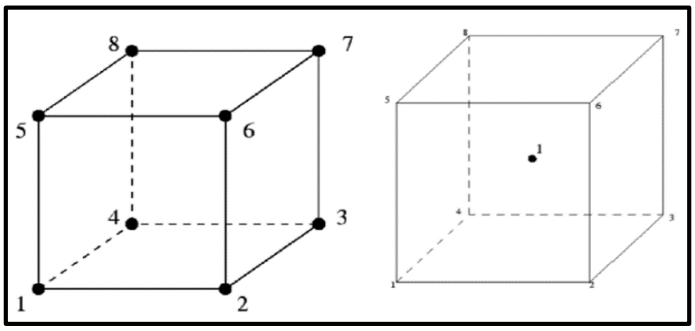

Figure 5. 8-node brick element with the integration point.

3.1.2 Modeling of steel reinforcement

Several models were used to model the steel reinforcement, such as solid, beam or truss elements. Because the reinforcing bars do not provide a very high bending stiffness, truss element is used. This element provided a perfect bond between concrete and steel bars during analysis. A linear 3D two-node truss element with three degrees of freedom at each node (T3D2) is used to model the steel reinforcement, **(CAE Abaqus, User's Manual, 2011)**. **(see Fig. 6)**.

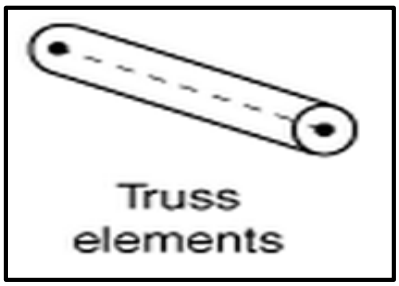

Figure 6. 3D two-node truss element (T3D2)

3.1.3 Modeling of steel fiber

Adding steel fiber to the concrete mixes lead to increase tensile and flexural strength, **(Cho and Kim, 2003)** and **(Tlemat, et al., 2006)**. For this reason, the modeling of steel fiber is very important for obtaining results matched with the experimental results. There are many models used to describe the stress-strain response in tension as shown in **Fig. 7**. In this study, the bilinear curve was used to model the fibered steel-concrete **(Wang and Hsu, 2001)**.

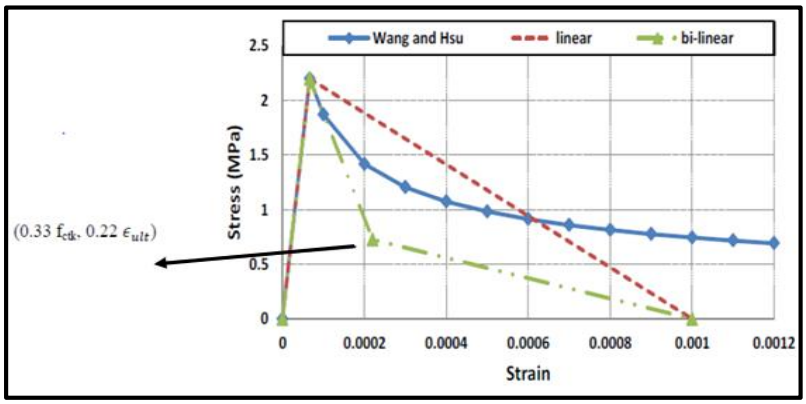

Figure 7. Uniaxial tensile stress-strain behavior of concrete

3.2 Input Data

The beams selected from experimental work are LS12 and SF12. The parameters obtained from laboratory tests such as compressive strength and splitting tensile strength were used in this program. For other parameters needed, such as dilation angle, eccentricity, $\boldsymbol{\sigma bo/\sigma co}$, kc, and viscosity parameter, ABAQUS default data were used. The value of fractions between concrete and supports obtained after many trails to reach the number that reduces the difference between the experimental and finite element results. This value was assumed 0.2. The input data of beams LS12 and SF12 are summarized in **Table 3**.

Table 3. Input data of beams LS12 and SF1.

Parameters	LS12	SF12
Compressive strength	49.32 MPa	43.22 MPa
Splitting tensile strength	6.13 MPa	5.77 MPa
Modulus of elasticity of concrete	34800 MPa	33750 MPa
Poisson's ratio of concrete	0.2	
Area of steel reinforcement, Ø4mm, Ø6mm (mm^2)	12.56, 28.27	
Yield strength, Ø4mm, Ø6mm (MPa)	565, 520	
Modulus of elasticity of steel reinforcement, Ø4mm, Ø6mm (MPa)	200000	
Poisson's ratio of steel reinforcement	0.3	

3.3 Three Dimensional Finite Element Meshes

The beam was meshed (divided) into a number of small finite elements with maximum size 30 mm as shown in **Fig. 8**; also the modeling of steel reinforcement is shown in **Fig. 9**. The beam was simply supported at both ends. One support was modeled as a roller by constraining in Y-direction (UY=zero), another support was modeled as a hinge by constraining in X, Y, and Z-direction (UY=UX=UZ= zero) as shown in **Fig. 10**. The beam was subjected to 12 mm displacement condition for monotonic loading. For repeated loading the beam was subjected to displacement equal to displacement obtained from monotonic test (experimental program).

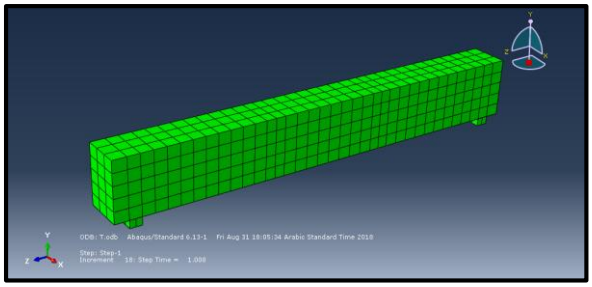

Figure 8. The finite element meshes

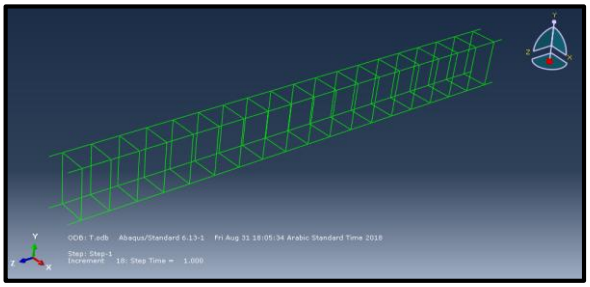

Figure 9. Modeling reinforcement

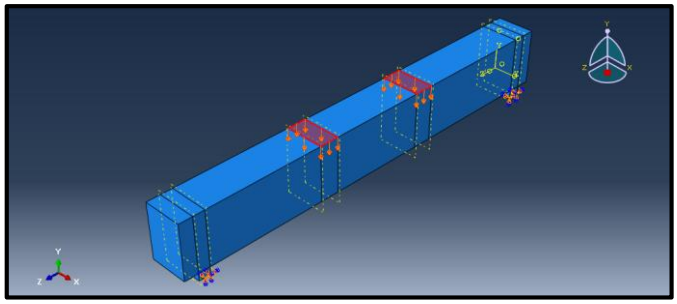

Figure 10. Boundary conditions

4. RESULTS AND DISCUSSION

4.1 Experimental Results

4.1.1 Fresh properties

The results of all mixes showed that the diameter of slump flow, time of V-funnel, and the blocking ratio of L-box belong under acceptance criteria for the European guideline. The workability of steel fiber reinforced self-compacting concrete mix (RSCC) decreased because of the presence of micro steel fibers. This reduction in workability due to steel fiber obstructs the movement of the mix and increases the friction between aggregate and fibers. It was also noticed that the workability decreased by adding different percentages of rubber. This diminution in workability is due to the low specific gravity of rubber particles relative to the specific gravity of other materials (coarse aggregate, fine aggregate, limestone dust, and silica fume). This leads to low mobility of mixes. The water to cement ratio (w/c) and VMA dosage increased by adding micro steel fibers and rubber particles. Therefore, all mixes satisfy the acceptance limits of the European guideline. The reduction in workability includes decrease in slump flow diameter, an increase in flow time, and a decrease in blocking ratio (H_2/H_1). The results of fresh properties are presented in **Table 4**.

Table 4. Results of fresh concrete tests.

Mixture	Slump Flow (mm)	V-Funnel test (sec)	L-box tests H_2/H_1
SCC	680	24	0.77
RSCC	677	24	0.76
CA20	630	27	0.75
CA10	641	26	0.76
FA20	643	26	0.75
FA10	650	26	0.75
LS50	660	26	0.76
LS25	665	25	0.77
LS12	668	25	0.77
SF50	670	25	0.76
SF25	675	24	0.77
SF12	676	24	0.77
EFNARC (2005)	**550-850 mm**	**7-27 sec**	**≥ 0.75**

4.1.2 Hardened properties

The results showed that the compressive strength was decreased as rubber content increased. The reduction in compressive strength about 37.1%, 11.4%, 41.8%, 14.7%, 16.8%, 39.0%, and 10.5% for mixes CA20, CA10, FA20, FA10, LS50, SF50, and SF25, respectively compared with reference mix (RSCC). The reason for this reduction is due to the soft particle of waste tire rubber compared with particle of aggregates or other materials. The adhesion between rubber and cement paste is weak (poor strength of the interfacial transition zone between the rubber particles and cement paste). Also, the reduction in splitting tensile strength and flexural strength attributed to the same reasons affected the compressive strength. The compressive strength was increased about 14.4%, 15%, and 28% in SF12, LS25, and LS12, respectively. **Table 5** shows the results of hardened concrete tests.

Table 5. Results of hardened concrete tests.

Mixes	Compressive strength (MPa)	Splitting strength (MPa)	Modulus of rupture (MPa)
SCC	35.01	4.07	6.53
RSCC	38.52	4.32	7.29
CA20	24.21	3.54	5.47
CA10	34.14	4.19	5.50
FA20	22.42	3.41	4.08
FA10	32.86	4.15	5.31
LS50	32.04	4.82	5.12
LS25	44.05	5.79	5.83
LS12	49.32	6.13	6.31
SF50	23.48	3.21	4.74
SF25	34.46	4.15	5.50
SF12	43.22	5.77	6.81

4.1.3 Flexural test results of beams

The results acquired from the flexural testing of the beams are illustrated in **Table 6**. The crack pattern of all the beams indicates that the failure mode of the beams is a flexural failure mode **(Fig. 11)**. During the first stage of testing, small perpendicular cracks formed in the mid-span of all the beams. The number of these cracks was increased when the applied load increased. The results observed that the width of the crack reduces by adding steel fiber and rubber particles due to the micro steel fiber block these cracks and restricted their widening **(Al-Quraishi, et al., 2017)** and (**Muhsin and AbdElzahra, 2016)**, also the capacity of rubber particles to absorb higher energy. The flexural stiffness can be defined as the slope of the load-deflection relation ($K= \Delta F/\Delta\delta$). The addition of micro steel fiber improves the flexural stiffness values and reduces the beam deformability, but these values decreased as rubber contains an increase. The decrease in K value is due to the lower modulus of elasticity of rubber particles (improve deform capacity).

Table 6. Results of flexural test.

Beam no.	Beam designation	Failure type	Load at first crack (kN)	Deflection at first crack (mm)	Flexural stiffness (mm)/(kN)		Load at failure (kN)	Deflection at failure (mm)	Number of crack at Failure	Crack width (mm)
B1	SCC	Flexural	14	1.73	8.09		21.99	7.60	6	0.06-0.20
B2	RSCC	Flexural	16	0.43	37.21		28.81	5.29	6	0.01-0.06
B3	CA20	Flexural	15	1.56	9.62		27.67	9.38	8	0.06-0.16
B4	CA10	Flexural	20	1.73	11.56		28.81	6.52	6	0.01-0.04
B5	FA20	Flexural	8	0.95	8.42		22.56	7.73	6	0.04-0.18
B6	FA10	Flexural	17	1.47	11.56		27.67	6.34	7	0.04-0.10
B7	LS50	Flexural	14	0.86	16.28		28.81	6.86	6	0.01-0.08
B8	LS25	Flexural	15	0.69	21.74		28.24	5.64	6	0.02-0.06
B9	LS12	Flexural	16	0.86	18.60		29.37	5.64	6	0.02-0.06
B10	SF50	Flexural	13	0.74	17.57		19.45	4.83	6	0.01-0.04
B11	SF25	Flexural	14	0.69	20.29		25.97	5.13	8	0.02-0.06
B12	SF12	Flexural	15	0.60	25.11		27.67	6.21	8	0.04-0.18

Figure 11. Beams after testing.

The results showed that the addition of steel fiber in B2 improves the failure load by about 31% compared to B1 but by adding rubber particles. This percentage dropped nearly 4% in B3, B6, and B12, also decreased approximately 21.7%, 2%, 32.5%, and 9.8% in B5, B8, B10, and B11, respectively. The results also showed improved failure loads in B9 about 2% compared to B2. The presence of steel fiber and waste tire rubber convert behavior of beams from brittle to ductile as shown in **Fig. 12**. Ductility can be defined as the ability of the structural member to undergo plastic zone before failure (area under the load-deflection curve between first crack and peak failure load). For all beams the ductility value increase as rubber content increase except in B10, B11, and B12. The addition of steel fiber and silica fume lead to increase ductility (post crack resistance), **(Nili and Afroughsabet, 2010)**.

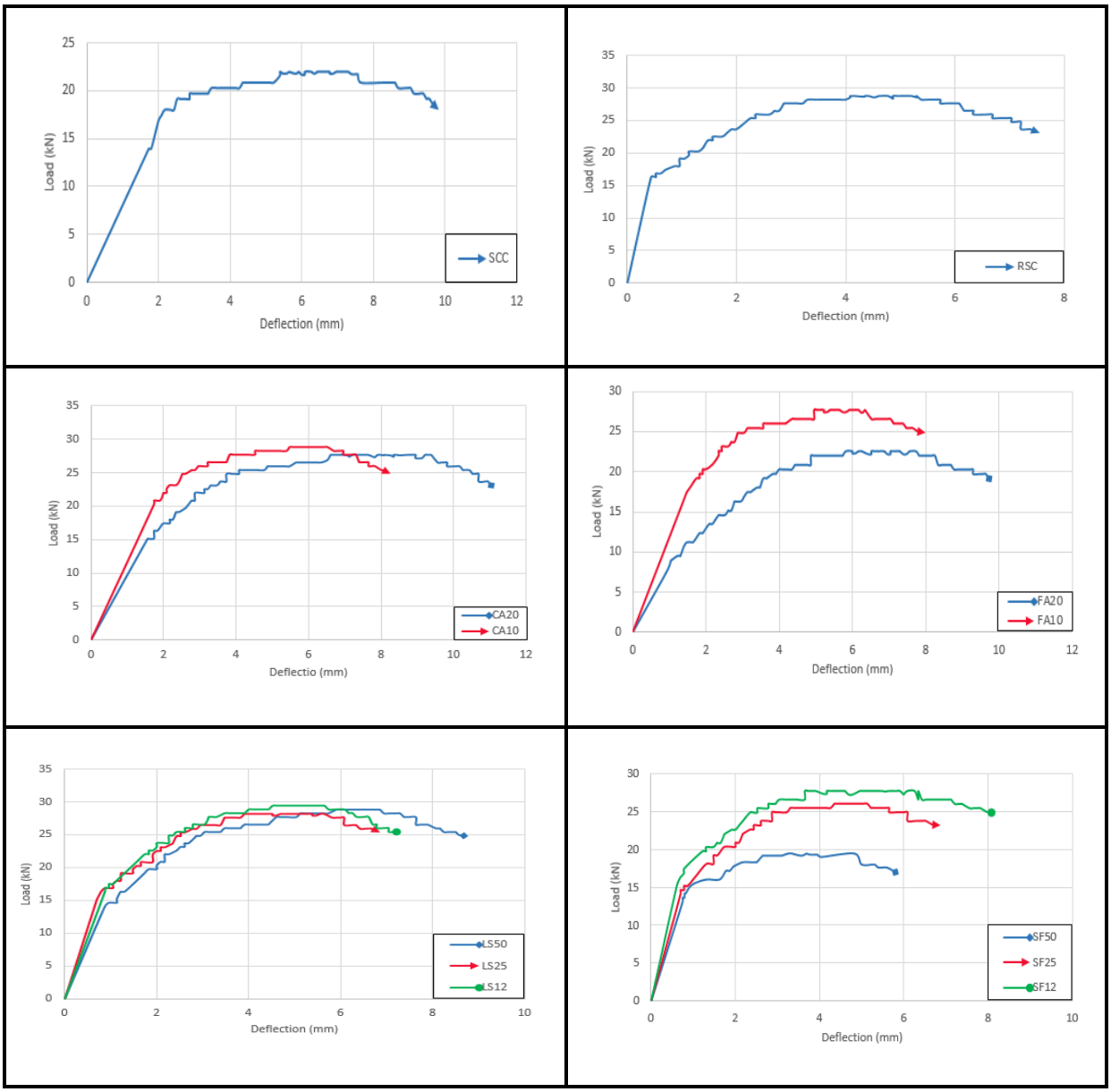

Figure 12. Load-deflection curves (Experimental).

Toughness indices and residual strength factors were also computed according to **(ASTM C1018-97)**. Toughness indices (I_5, I_{10}, and I_{20}) increase as rubber content increases due to the lower stiffness (increase flexibility and energy absorption). Residual strength factors, which are derived directly from toughness indices. It means the level of strength retained after first crack. Micro steel fibers and rubber particles increase residual strength factors. **Table 7** presents the ductility values, toughness indices, and residual strength factors.

Table 7. Ductility, toughness indices, and residual strength factors.

Beam no.	Beam designation	Ductility (kN.mm)	Toughness indices*			Residual strength factors**	
			I_5	I_{10}	I_{20}	$R_{5,10}$	$R_{10,20}$
B1	SCC	121.2	6.1	14.0	***	158	***
B2	RSCC	125.5	6.5	14.6	30.1	162	155
B3	CA20	199.5	7.1	15.9	32.3	176	164
B4	CA10	132.7	6.5	12.4	***	118	***
B5	FA20	128.4	8.2	20.7	47.8	250	271
B6	FA10	126.6	6.7	14.8	31.3	162	165
B7	LS50	150.9	7.3	15.9	35.3	172	194
B8	LS25	128.1	7.1	15.3	33.6	164	183
B9	LS12	126.4	6.9	15.0	30.4	162	156
B10	SF50	80.1	6.3	13.1	30.3	136	172
B11	SF25	102.8	6.5	15.1	32.7	172	176
B12	SF12	144.0	6.9	16.2	33.1	186	169

*(I_5, I_{10}, and I_{20}): the value computed by dividing the area at deflection of 3.0, 5.5, and 10.5times the first crack deflection by the area at first crack deflection.
** $R_{5,10} = 20 (I_{10} – I_5)$, $R_{10,20} = 10 (I_{20} – I_{10})$
***These value could not be calculated because the curve readings were few

4.2 Finite Element Analysis Results

4.2.1 Monotonic loading

The numerical analysis results for beams LS12 and SF12 under monotonic loading are illustrated in **Table 8**. This table also presents the different percentages between experimental and numerical analysis results. The comparison between the numerical and experimental load-deflection curves are presented in **Fig. 13**. An acceptable agreement can be noticed from this figure.

The ultimate load obtained from FEA is higher than the ultimate load obtained from experimental work. This is due to the right modeling of steel fibers (tension stiffening). Also, it is due to the rubber effect, which represents increasing compressive strength (49.32 MPa and 42.22 MPa) only without taking into account the change in structure of concrete. The structures of the concrete greatly affect the behavior of the beams in experimental work. The ultimate load obtained from finite element analysis was 32.70 kN with central- deflection 6.14 mm and 31.08 MPa with the central-deflection 6.01 mm for LS12 and SF12, respectively. The different percentages between experimental and numerical analysis results were 7.93% and 12.32% for ultimate load, 8.87% and -2.89% for mid-span deflection for LS12 and SF12, respectively. **Fig. 14** and **Fig. 15** shows the deformation shape and crack pattern for these beams respectively.

Table 8. Numerical analysis results of the tested specimens.

Modeled beam	Ultimate load (kN)			Mid span deflection (mm)		
	EXP.	F.E	% of variation	EXP.	F.E	% of variation
LS12	29.37	31.70	7.93%	5.64	6.14	8.87%
SF12	27.67	31.08	12.32%	6.21	6.03	-2.89%

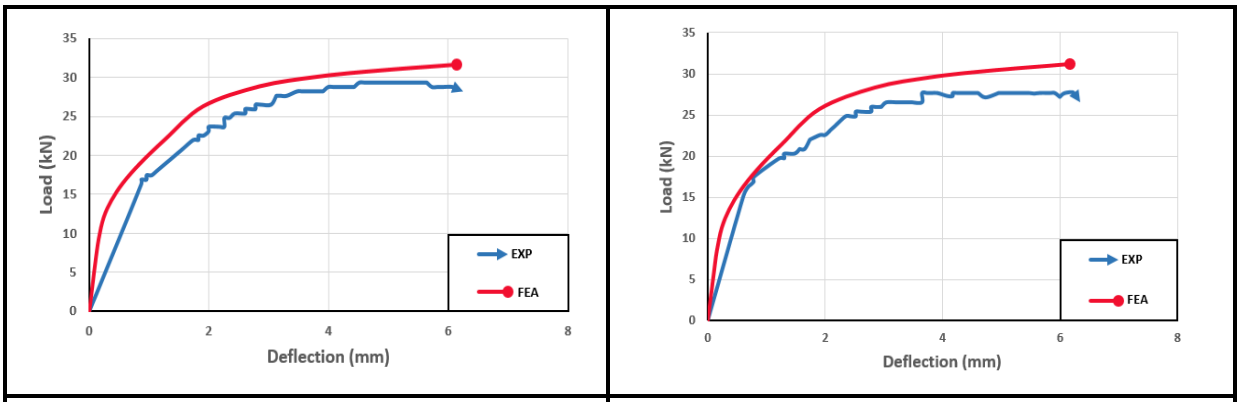

Figure 13. Numerical and experimental Load-deflection curves.

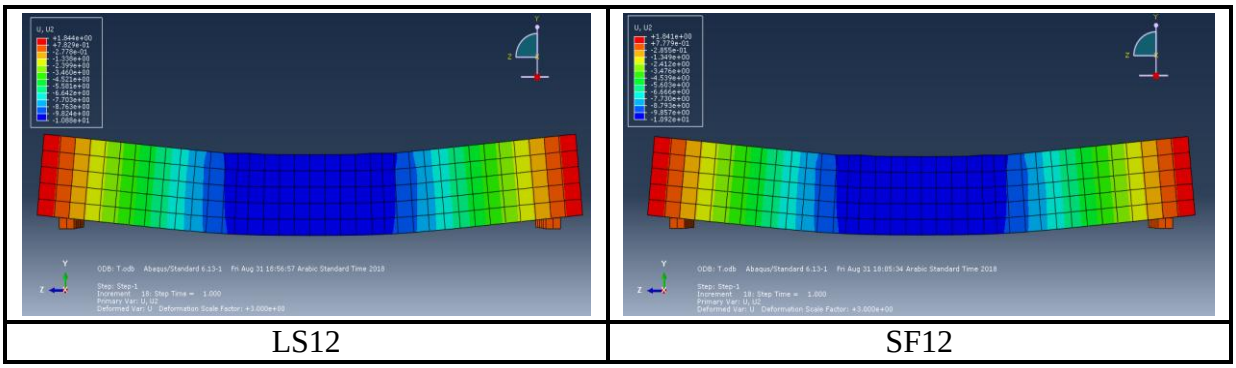

Figure 14. Deformation shape.

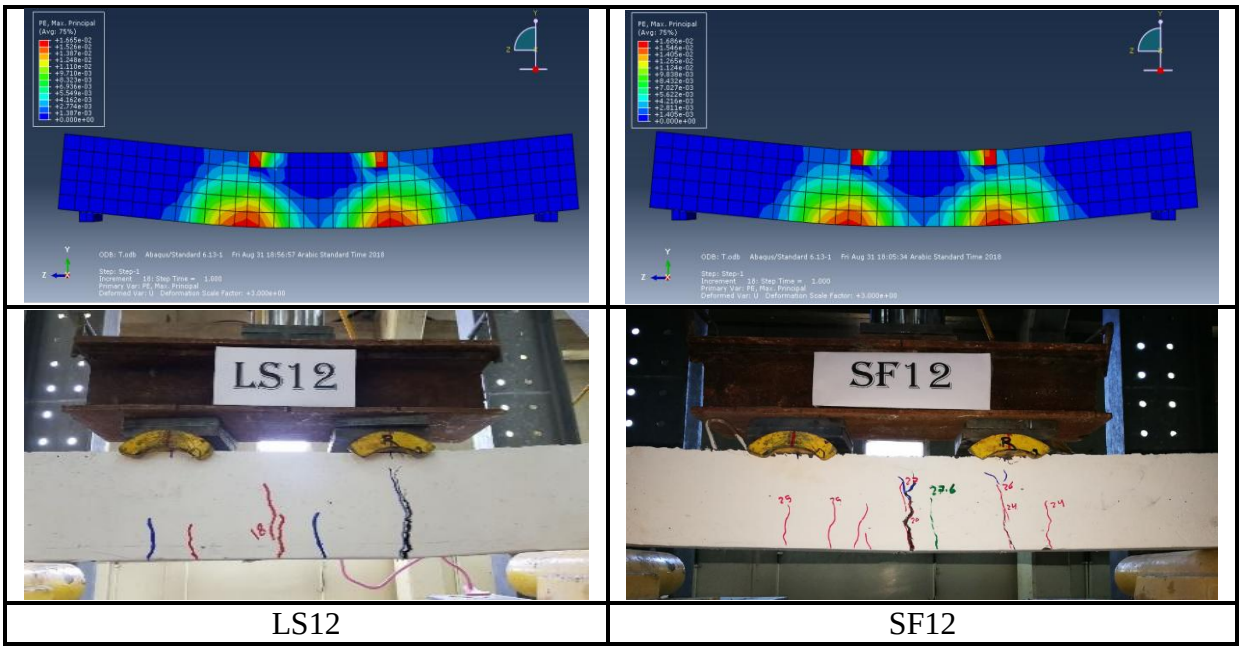

Figure 15. Crack pattern.

4.2.2 Repeated loading

The load history (cyclic load), as shown in **Fig. 16** was applied to the specimens (LS12 and SF12). This load history was recommended by **(FEMA, 2007)**.

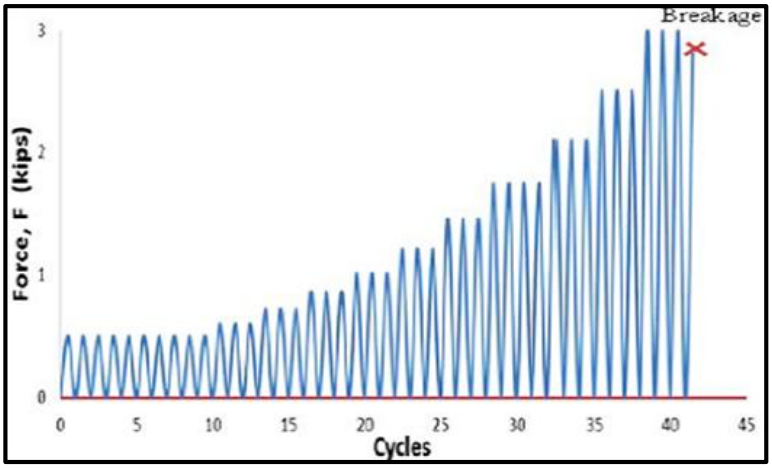

Figure 16. Load history used in FEA.

The numerical analysis results for beams LS12 and SF12 under repeated loading are illustrated in **Table 9**. This table also presents the different percentages between monotonic and repeated results (FEA). The load-mid span deflection relation obtained from numerical analysis by ABAQUS under monotonic and repeated loading is presented in **Fig. 17** of beams LS12 and SF12. **Fig. 18** shows the deformation shape of these beams.

Table 9. Comparison between monotonic and repeated loading (FEA)

Modeled beam	Monotonic loading		Repeated loading		% of variation	
	Ultimate load (kN)	Deflection at ultimate load (mm)	Ultimate load (kN)	Deflection at ultimate load (mm)	Ultimate load (kN)	Deflection at ultimate load (mm)
LS12	31.70	6.14	31.12	7.43	- 1.83%	21.01%
SF12	31.08	6.03	30.14	6.95	- 3.02%	15.26%

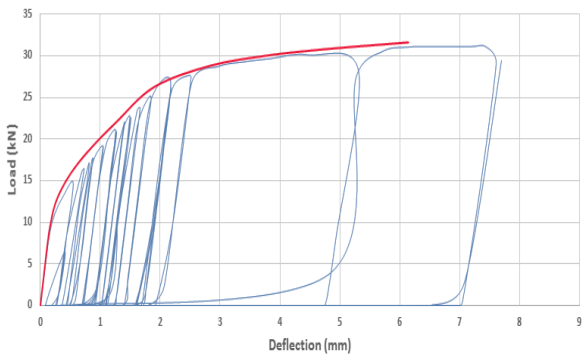

LS12

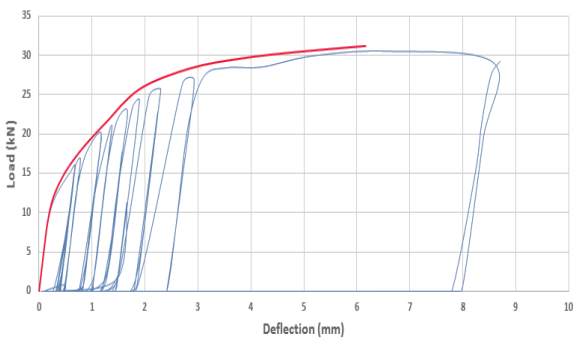

SF12

Figure 17. Numerical load-deflection curve for monotonic and repeated FEM loads.

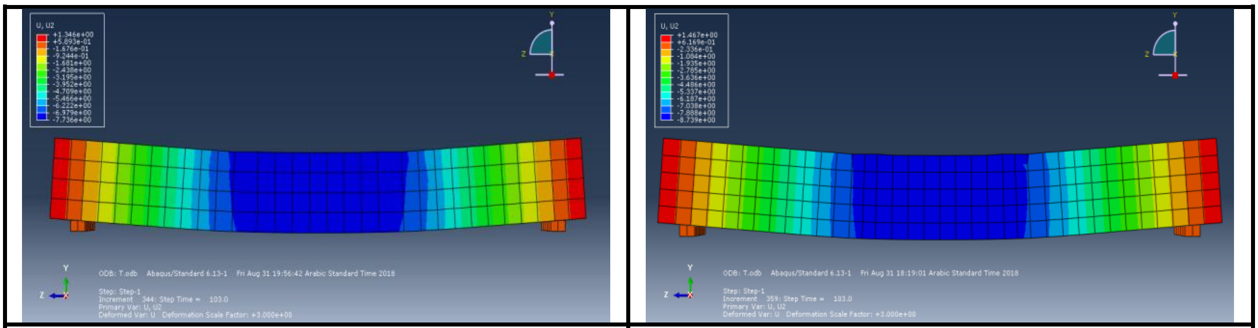

LS12	SF12

Figur18. Deformed shape (FEM).

Table 9 and **Fig. 17** shows that the differences between the results of monotonic loading and repeated loading (ultimate load) were insignificant differences. The addition of steel fibers improves the load-bearing capacity under repeated loading with large strain before failure, **(Jun and Stang, 1998)**. The load-deflection curve (FEA monotonic test) showed the ductile behavior of beams LS12 and SF12, therefor the ultimate load obtained from repeated loading is close to the ultimate load obtained from monotonic test. The percentage of difference between the ultimate loads obtained from monotonic and repeated loading about 1.83% for LS12 and 3.02% for SF12. Also the different percentages between the deflections at ultimate load about 21.01% for LS12 and 15.26% for SF12.

5. CONCLUSIONS

These conclusions were obtained on the basis of the results obtained by testing the specimens: The fresh properties of SFRSCRC decreased as rubber content increased. The engineering properties decreased with increased rubber content when rubber used as aggregates but these properties increased when rubber used as filler materials. Flexural stiffness and load at failure decreased when the percentage of waster tire rubber increased, for all beams. The results observed that the deformability, ductility, and toughness indices increased with rubber content increased. The failure mode of the tested beams converts from brittle to ductile by adding rubber particles and micro steel fibers. The optimum percentage of rubber replacement was 10% for coarse and fine aggregate, and 12% for limestone dust and silica fume (depended on the results of fresh properties, hardened properties, and behavior of beams). The results obtained from FEA by using ABAQUS program showed that acceptable percentages of differences between the numerical analysis results and the experimental results. The percentages of differences between beams LS12 and SF12 was 7.93% and 12.32% for ultimate load, 8.87% and -2.89% for deflection at ultimate load (monotonic loading). Insignificant ultimate load differences between the results of monotonic loading and repeated loading. The percentage of difference between the ultimate loads obtained from monotonic and repeated loading was about 1.83% for LS12 and 3.02% for SF12.

6. REFERENCES

- ACI 318, 2014. Building Code Requirements for Structural Concrete and Commentary. *American Concrete Institute*, Farmington Hills, MI, USA.

- Al-Quraishi, H., Ghanim, G., and Asaad, Z., 2017. Compressive Strength of Bottle-Shaped Compression Fields of Fiber Reinforced Concrete Members. *Journal of Engineering*, *23*(11), pp., 56-69.

- ASTM A496, 2002. Standard Specification for Steel wires, Deformed, for Concrete Reinforcement. *ASTM International*, West Conshohocken.

- ASTM C1018, 1997. Standard Test Method for Flexural Toughness and First-crack Strength of Fiber-reinforced Concrete. *ASTM International*, West Conshohocken.

- ASTM C1240, 2015. Standard Specification for Silica Fume Used for Cementitious Mixtures. *ASTM International*, West Conshohocken.

- ASTM C496, 2011. Standard Method of Test for Splitting Tensile Strength of Cylindrical Concrete Specimens. *ASTM International*, West Conshohocken.

- ASTM C78, 2002. Standard Test Method for Flexural Strength of Concrete Using Simple Beam with Third-Point Loading. *ASTM International*, West Conshohocken.

- BS1881-116, 1997. Method for Determination of Compression Strength of Concrete Cubes. *British Standard Institute*, London.

- CAE Abaqus. User's Manual. 2011. Abaqus analysis user's manual.

- Chaudhari, S. V., and Chakrabarti, M. A., 2012. Modeling of Concrete for Nonlinear Analysis Using Finite Element Code ABAQUS. *International Journal of Computer Applications*, 44(7), pp., 14-18.

- Cho, S. H., and Kim, Y. I., 2003. Effects of Steel Fibers on Short Beams Loaded in Shear. *Structural Journal*, 100(6), pp., 765-774.

- De Brito, J., and Saikia, N., 2012. *Recycled Aggregate in Concrete: Use of Industrial, Construction and Demolition Waste*. New York: Springer Science and Business Media.

- EFNARC, 2005. The European guidelines for self-compacting concrete, Production, and use.

- FEMA, A., 461/Interim, 2007. Testing Protocols for Determining the Seismic Performance Characteristics of Structural and Nonstructural Components. *Applied Technology Council*, Redwood City, CA, 113.

- Ganesan, N., Raj, J. B., and Shashikala, A. P., 2013. Behavior of Self-Consolidating Rubberized Concrete Beam-Column Joints. *ACI Materials Journal*, 110(6), pp., 697-704.

- Iraqi specification No. 45, 1984. Aggregate from natural source for concrete. *Central Agency for Standardization and Quality Control, Planning Council*, Baghdad, Iraq.

- Ismail, M. K., and Hassan, A. A., 2016. Performance of Full-Scale Self-Consolidating Rubberized Concrete Beams in Flexural. *ACI Materials Journal*, 113(2), pp., 1-12.

- Jun, Z., and Stang, H., 1998. Fatigue performance in flexure of fiber reinforced concrete. *Materials Journal*, *95*(1), pp., 58-67.

- Matar, P., and Assaad, J. J., 2019. Concurrent Effects of Recycled Aggregates and Polypropylene Fibers on Workability and Key Strength Properties of Self-consolidating Concrete. *Construction and Building Materials*, *199*, pp. 492-500.

- Muhsin, M. H., and AbdElzahra, I. H., 2016. Studying the Combination Effect of Additives and Micro Steel Fibers on Cracks of Self-Healing Concrete. *Journal of Engineering*, *22*(1), pp., 49-67.

- Najim, K. B., and Hall, M., 2014. Structural Behaviour and Durability of Steel-Reinforced Structural Plain/Self-Compacting Rubberised Concrete (PRC/SCRC). *Construction and Building Materials*, 73, pp., 490-497.

- Nili, M., and Afroughsabet, V., 2010. Combined Effect of Silica Fume and Steel Fibers on the Impact Resistance and Mechanical Properties of Concrete. *International Journal of Impact Engineering*, 37(8), pp., 879-886.

- Padhi, S., and Panda, K. C, 2016. Fresh and Hardened Properties of Rubberized Concrete Using Fine Rubber and Silpozz. *Advances in Concrete Construction*, 4(1), pp., 49-69.

- Tlemat, H., Pilakoutas, K., and Neocleous, K., 2006. Modeling of SFRC Using Inverse Finite Element Analysis. *Materials and Structures*, 39(2), pp., 221-233.

- Wang, T., and Hsu, T. T., 2001. Nonlinear finite element analysis of concrete structures using new constitutive models. *Computers & Structures*, 79(32), pp., 2781-2791.

NOMENCLATURE

EFNARC= European Federation of National Trade Associations Representing Concrete
FEM= Finite Element Method
SCC= Self-Compacting Concrete
SCRC= Self-Compacting Rubberized Concrete
SFRSCRC= Steel Fiber Reinforced Self-Compacting Rubberized Concrete
VMA= Viscosity Modifying Admixture
$\boldsymbol{\sigma bo}/\boldsymbol{\sigma co}=$ Ratio of the initial equibiaxial compressive strength to the uniaxial compressive strength
Kc=Ratio of the second stress invariant on the tensile stress meridian to the second stress invariant on the compressive stress meridian